Sustainable Electrodes for the Next Generation of Redox Flow Batteries

Michael W. Thielke[1,*], Gengyu Tian[1] and Ana Jorge Sobrido[1,*]

[1] School of Engineering and Materials Science, Queen Mary University of London, London, United Kingdom

E-mail: a.sobrido@qmul.a.c.uk

Received xxxxxx
Accepted for publication xxxxxx
Published xxxxxx

Abstract

The development of alternative energy storage technologies is key to advance renewable energy resources. Among them, redox flow batteries have been identified to be one of the most promising technologies in the field of stationary batteries. The carbon-based electrodes in these batteries are a crucial component and play an important part in achieving high efficiency and performance. A further leap into this direction is the design of fossil-free materials by incorporating sustainable alternative resources as the carbon component in the processing of the electrodes. The use of biomass as carbon precursor for electrode applications has also been a focus of research for other energy storage devices and in the case of redox flow batteries, it has become an emergent topic in recent years. This short review presents the recent advances in the design of biomass-derived carbon materials as electrodes in redox flow batteries, strategies to enhance their electrocatalytic properties, challenges, and future outlook in the design of sustainable electrode materials.

Keywords: sustainable material, redox flow battery, electrode, biomass

1. Introduction

The 2021 report published by the Intergovernmental Panel on Climate Change (IPCC) confirmed what it has been monitored closely for the last few years: that greenhouse gas concentration in the atmosphere has reached unseen levels for humankind.[1] In particular, carbon dioxide averages at 410 ppm, the highest concentration in at least 2 million years, with a shocking 47% increase since 1750. Moreover, the global surface temperature has increased faster in the last 50 years than in any other period over the last 2000 years. These numbers highlight the urgent need for sustainable and renewable resources to end the dependency of our energy supply on finite fossil fuels. At the same time, if we want to be able to rely on renewable resources, new solutions to energy storage must be developed, so an efficient balance of the inherently intermittent renewable energy can be achieved in order to ensure a seamless energy coverage at any given time. In recent years, particular efforts have been devoted to electrochemical energy storage technologies, i.e. batteries, due to their flexibility to operate in a variety of scenarios of electric power and energy capacity requirements. Among the most promising candidates for grid-scale energy storage are the redox flow batteries (RFBs). Many redox flow batteries with multiple chemistries have been reported over the last decade, including iron-chromium flow batteries,[2, 3] zinc-based flow batteries[4, 5] (zinc-bromide, Zn-Cl, Zn-Air, zinc-polyiodide[6]), and polysulfide bromide flow batteries, but perhaps the most popular is the all-vanadium redox flow battery (VRFB) (**Figure 1**), reaching worldwide application at industrial scale. Both anolyte and catholyte employ vanadium ions with different oxidation states (V^{2+}, V^{3+}, VO^{2+}, and VO_2^+), minimizing the crossover effect, common cause of failure and decrease in performance of RFBs.

One unique feature of RFBs is that power and energy are decoupled, enabling customization of the energy capacity at a

given power by increasing the size of the electrolyte tanks or the concentration of redox active species in the electrolyte. Anolyte and catholyte are pumped through half-cells, separated from each other by an ion-exchange membrane. The electrodes, commonly carbon felts or papers, are a crucial component of the RFBs and their chemical and physical properties play a major role in both performance and durability of the battery.[7, 8] The most common RFB carbon electrodes are based on carbonized polyacrylonitrile (PAN) fibers, due to their wide range of operating potential, high conductivity and high chemical resistance. They are commercialized in the form of papers and felts, exhibiting a stable 3D fibers network with a relatively high surface area, which undergo low-pressure loss from the circulating electrolytes without compromising the available surface area. However, PAN-derived carbon electrodes exhibit low activity towards redox reactions and poor wettability, which in turns lead to low performances.[9] Approaches such as thermal activation,[10] plasma activation,[11] or (electro)chemical activation[12-15] enhance the hydrophilicity of the electrode surface, increasing wettability and providing functional groups as active sites for electron transfer. Nevertheless, there are still obvious structural and compositional limitations associated to commercial materials, along with the fact that they derive from non-sustainable resources.

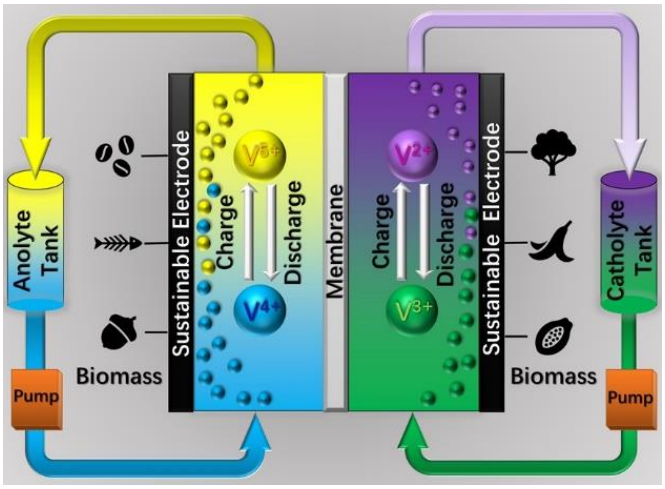

Figure 1 Schematic representation of VRFB working principle with biomass-derived carbon electrodes.

Biomass-derived materials stand as a fantastic source to produce sustainable carbon fibers for energy storage applications. Carbonized rayon fibers, which are synthetically made from regenerated cellulose, are the most common source for carbon electrodes after PAN.[8, 16] Most man-made cellulosic fibers are produced *via* the viscose process, which includes the use of harsh chemicals. However, greener alternatives, such as the use of ionic liquids as solvents and recycled cotton waste, have showed promising results, but have not made it to commercialization, yet.[17, 18] Alternative carbon sources from biowaste have been proposed to be competitive *versus* commercial PAN-derived felts, achieving comparable and even higher performance, in a more sustainable way. The choice of carbon sources from biomaterials has great influence on the properties of the resulting carbon, particularly in terms of heteroatom doping and graphitic carbon content. Unlike PAN, elements different than nitrogen can dope the carbon structure, the most common being nitrogen,[19, 20] oxygen,[21] phosphorus,[22, 23] and sulphur.[24] Most of the reported electrodes based on the use of biomaterials still involve the use of carbon felts as support, although there have been some recent promising attempts to develop freestanding biomass-derived electrodes for RFBs.[25-27] In any case, the number of publications in the field of biomass-derived electrodes has been steadily increasing over the last few years. In this short review, we would like to showcase some of the efforts to produce sustainable high-performing electrode materials for RFBs conducted over the last five years and suggest new avenues for further research.

2. Sustainable electrodes for redox flow batteries

Electrodes are a key component in any electrochemical device. In RFBs, in particular, electrodes must withstand the continuous flow of electrolyte that carries the redox active species that enable the storage of energy. They must possess a porous three-dimensional structure, high surface area, active sites for chemical reactions, and allow for efficient electrolyte transport. This is crucial to increase the rate capability and efficiency of the device.[28] They also need to exhibit high hydrodynamic permeability, high electric conductivity, chemical and electrochemical inertness, and be stable within a wide voltage window.[29] Carbon in the form of fibers has been proven to fulfil these criteria. The main source for carbon electrode materials today and in the past has been based on PAN. However, recently more attention has been devoted to the research of biomass-derived materials as alternative to petrol-derived carbons.[30, 31]

The processing of biomass into carbon materials for energy typically involves a carbonization or pyrolysis step followed by an activation step (physical or chemical procedure such as thermal, hydrothermal, acid treatment) to achieve high surface area and improved electrocatalytic properties.[32] Depending on the source of the initial biomaterial, a variety of compositions, porous structures and morphologies can be produced. Additionally, the use of additives, such as amines, urea, phosphoric acid, or for example, iron containing additives can lead to the introduction of heteroatoms to boost the performance of the biomass-derived carbon electrodes.[33] These strategies lead to an increase of charge accumulation at the interface electrode / electrolyte, which in turns promotes

the adsorption of positive and negative charges to the surface of the electrode.[34, 35]

2.1 Boosting activity of carbon felts via decoration with biomass-derived carbon electrocatalysts

One approach to enhance the electrocatalytic activity of carbon felts is the deposition of carbon with electrocatalytic properties, often leading to an increase of surface area and electrocatalytic activity. A schematic synthesis route of the process is shown in **Figure 2**. These carbon-based electrocatalysts include activated carbon,[36] carbon nanofibers,[37] carbon aerogels,[38, 39] graphene,[40-42] graphene oxide (GO),[43] reduced graphene oxide (rGO),[44, 45] carbon nanotubes,[46, 47] carbon microspheres,[48] or carbon nanorods.[49] Activated carbon (AC) has been widely researched as electrode because of its high porosity, electrical conductivity, and stability in acidic media, enabling it to provide more active sites for electrocatalytic reactions.[50, 51] Wan *et al.* reported AC extracted from chitin (shrimp shell) and pine wood in a direct comparison showing the influence of different precursors that have been treated following the same hydrothermal process at 200 °C or 300 °C followed by carbonization at 850 °C in nitrogen.[52] The hydrothermal temperature was reported to have an important effect on the Brunauer-Emmett-Teller (BET) surface of area, particularly for the chitin AC, with 616 m^2 g^{-1} for the 200 °C and 102 m^2/g for AC produced at 300 °C. The electrochemical surface area (ECSA) for the sample prepared at 200 °C was more than double than that of the 300 °C material. Cyclic voltammetry (CV) and ECSA measurements performed in 1 M V^{2+}, 2 M H_2SO_4 or 0.1 M $VOSO_4$ in 0.1 M H_2SO_4 indicated a much higher overall activity of the chitin-based AC compared to the pine wood AC, attributed to the presence of N in chitin. The chitin AC prepared at 200 °C exhibited the highest performance for both electrolytes tested including the performance of the chitin AC prepared at 200 °C with respect to the one prepared at 300 °C due to the higher surface area and the abundance of active sites, rather than to the elemental composition of those active sites, as both chitin AC contained similar amounts of nitrogen. The chitin AC prepared at 200 °C deposited on carbon felt *via* a passive flow method, led to a significant improvement of the kinetics and obtained a maximum power density of 438 mW cm^{-2}. Electrochemical impedance spectroscopy (EIS) measurements of the electrodes at higher frequency also revealed faster kinetics for the chitin sample prepared at 200 °C, and a decrease in mass transport resistance. The overall higher performance can directly be attributed to the higher resulting ECSA for the chitin AC compared to the pine wood one.

A different approach for the fabrication of AC using fresh sal wood sawdust consisted of a hydrothermal treatment in the presence of $ZnCl_2$ to promote the formation of oxygen functionalities and porosity on the surface.[53] The hydrothermal product was carbonized at 850 C under nitrogen, leading to the formation of a sawdust-derived AC with a BET-surface area of 1857 m^2 g^{-1}, of which 1280 m^2 g^{-1} consisted of mesopores with diameters between 2 and 50 nm, and C and O concentration of 96.4 at.% and 3.6 at.%, respectively. Cyclic voltammograms in 1.6 M $V^{3+/4+}$, 4.5 M H_2SO_4 as electrolyte of the sawdust-derived AC carbon felt exhibited anodic and cathodic peaks significantly higher than the ones of the pristine electrode, indicating improved electron transfer. EIS measurements also revealed lower ohmic and charge transfer resistances at the electrolyte/electrode interface, which were attributed to the oxygen functionalities present at the surface of the electrode. Charge-discharge studies showed energy efficiencies of around 90%, at current densities between 20 and 80 mA cm^{-2}, and long-term cycling test at 40 mA cm^{-2} over 50 cycles.

A comparable approach was conducted using orange peel as starting material. The AC was obtained by thermal treating the orange peel at 400 °C in argon, followed by an activation step consisting of carbonization and KOH treatment at 800 °C in argon.[54] The resulting AC exhibited a visibly high porous surface area of 1901 m^2 g^{-1}, as seen in **Figure 2**, and an oxygen-rich surface, leading to improved electrocatalytic properties and redox flow battery performance for the carbon felt electrodes with supported AC. The RFB performance remained stable after 100 cycles at 20 mA cm^{-2} current density.

KOH activation is a common method to drastically increase surface area in carbons. This approach was applied to used tea bags to produce carbon electrocatalysts for RFBs. BET surface areas of up to 2085 m^2 g^{-1} were obtained, increasing with increasing the KOH ratio. The modified graphite felt decorated with used tea bag-derived carbon exhibited steady charge-discharge cycles and improved capacity, voltage and energy efficiencies, compared to pristine graphite felt.[55]

Nanostructured porous carbon particles have also been produced from mature seeds of a deciduous tropical nut-bearing tree named scaphium scaphigerum, by soaking them in deionized water to expand in volume, followed by a hydrothermal treatment.[56] Its high surface area is ideal for the introduction of additives or heteroatoms into the forming porous carbon structure during the high temperature carbonization step under inert gas atmosphere. This way, iron doping was achieved by mixing the hydrothermal product with $FeCl_3$ and subsequent carbonization at 800 °C in argon, followed by HCl and water washing.[56] The addition of $FeCl_3$ led to a higher surface area for the resulting porous carbon

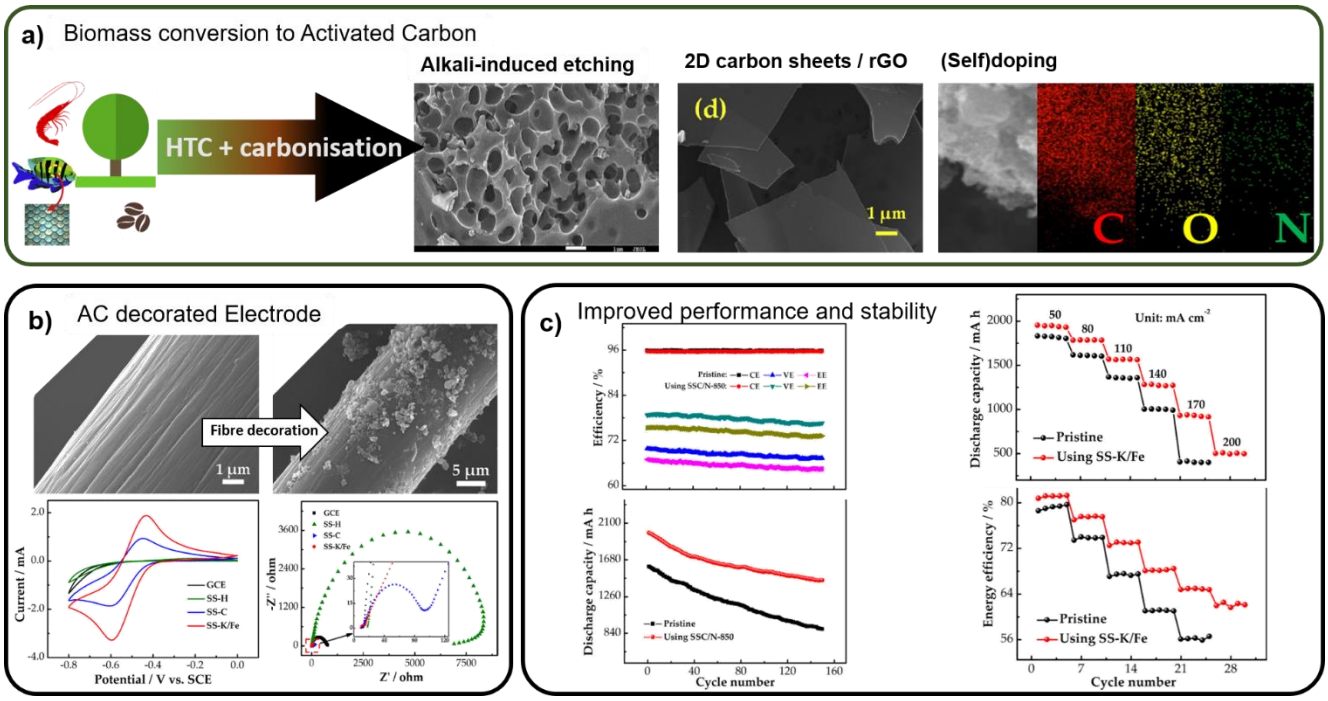

Figure 2 a) schematic depiction of the fabrication process of biomass-derived AC through HTC and carbonization in protective gas (N_2 or Ar). Depending on additives in the process, the morphology can be influenced to result into 2D structures (rGO[60] or 2D nano sheets[57]) or highly porous carbon structures as a result from alkali inducing surface etching, resulting in outstanding high surface areas (reported up to 1857[53], 1901[54], or 2085[55] m^2 g^{-1}). Self-doping in case of chitin-based biomass (shrimp[52], fish scales[57]) can be observed, or induced by additives to the carbonisation leading to doping with nitrogen[35, 58] or oxygen[55] or iron[59]. b) The AC can be used to decorate the fiber surface, enhancing the electrocatalytic properties, determined by CV or EIS. c) The modified GF electrodes are used in RFBs with enhanced performances in energy efficiency and capacity at different charge/discharge rates and in long term measurement.

(615.6 m^2 g^{-1} *versus* 259.8 m^2 g^{-1}). Additionally, a higher degree of graphitization was revealed by the higher static contact angle (139.6° to 120.1°), and the higher intensity ratio of G band to D band (I_G/I_D) (1.06 to 1.01) in Raman measurement. XPS showed that the content of C=C and C-C was 38.0% and 42.0%, respectively. Graphite felt with deposited Fe-doped C exhibited higher discharge capacity and energy efficiency than the pristine carbon felt when tested in a VRFB, at all current densities. At 100 mA cm^{-2}, the discharge capacity and energy efficiency of the VRFB with the Fe-doped C decorated graphite felts were 81.82 mA h^{-1} and 69.53%, higher than those of the pristine graphite felts.

Potassium ferrate (K_2FeO_4) was also reported to produce porous, oxygen-rich, high-graphitized carbon materials.[57] Due to the catalytic effect of K_2FeO_4, an increased graphitization and oxygen-deposition was achieved on the surface in a less time-consuming method that also led to a high activation efficiency. With a large specific surface area of 1086.9 m^2 g^{-1} (*vs* 262.3 m^2 g^{-1} without K_2FeO_4) and a higher degree of defects, the obtained Fe-doped carbon was used to decorate graphite felt**)**. The modified carbon fibers exhibited an improved electrocatalytic performance (**Figure 2**) shown in the CV at scan rates from 10 mV s^{-1} to 60 mV s^{-1} and lower charge transfer resistance and improved charge transfer in EIS measurements compared to a pristine graphite felt (**Figure 2**). The RFB cell with the modified felt as electrode exhibited an energy efficiency of 72.4% at 50 mA cm^{-2}, an improvement of 6.2% with respect to the pristine felt, and discharge capacity 11.1% higher.

Another very popular source of biomass-waste carbon is spent coffee grounds and have been the focus of several reviews.[58-60] Reduced graphene oxide (rGO) derived from spent coffee grounds has been reported as electrode material for RFBs.[61] The coffee grounds were washed and dried, then were carbonized at 850 °C in nitrogen for 2 (rGO-2) or 3 hours (rGO-3), chemically activated via modified Hummer's method to prepare graphene oxide,[62] then reduced by hydrazine monohydrate reduction to produce rGO,[63] obtaining BET surface areas of 72 m^2 g^{-1} for both rGO-2 and rGO-3. The rGO-3 sample presented 1% more O and rGO-2 1% more N determined by XPS, indicating higher reduction in the case of rGO-2. Both samples consisted of layers of graphite stacks, fine particles, and crumpled structures. The results indicated better performance of rGO-2 over rGO-3, attributed to higher electronic conductivity. However, the pristine graphite plate still showed the lowest potential difference for the V^{4+}/V^{5+}

redox pair (0.57 V vs 0.82 V) and comparable electrochemical performance for the V^{2+}/V^{3+} redox pair (0.57 V vs 0.61 V). Nevertheless, the reported reduced graphene oxide electrodes exhibited improved reversibility when compared to pristine graphite. When tested in a VRFB, using 1.6 M $V^{3.5+}$in 4 M H_2SO_4, the rGO-2 presented a slightly higher coulombic efficiency (CE) and slightly lower voltage efficiency (VE) than the pristine graphite electrode, resulting in a comparable energy efficiency (EE) overall, while all efficiencies were superior to its counterpart rGO-3. Overall, the authors demonstrated that the use of rGO from spent coffee beans is a promising strategy to enhance the electrocatalytic properties of graphite electrodes in RFBs, originating from a globally abundant biowaste, and performing at the same level than commercial bipolar graphite electrode. Other works used pyrolyzed coffee beans to form activated carbon with pyrolysis temperature of 850 °C followed by a steam-based activation. BET surface area increased with increasing activation time, while the yield decreased up to a surface area of 1113 m^2/g and 5.9% yield for the sample activated for 3h.[64] For electrochemical characterization, 60 µL cm^{-1} of a slurry (BC or AC, polyvinylidene fluoride (PVDF), and N-methyl-2-pyrrolidone (NMP)) was deposited on the surface of graphite plates and dried overnight. The CVs of the pyrolyzed coffee beans activated for 3h deposited onto graphite plate (AC3-GP) in 1.6 M $V^{3+/4+}$, 4 M H_2SO_4 were recorded and compare with the pristine graphite (GP) and non-activated biochar deposited onto graphite plate (BC-GP). BC-modified graphite plate electrodes exhibited better electrochemical performance, with higher anodic and cathodic peak currents for both redox couples than graphite. This result suggested an enhanced electron transfer process on both anode and cathode. A smaller peak potential separation for the V^{4+}/V^{5+} redox couple also suggested an improved reversibility. EIS data showed that AC3-GP electrode exhibited lower charge transfer resistance. However, the CV measurements showed lower redox current. This was attributed to possible trapping of electrolyte inside the microporous channels of the electrode. The VRFB assembled with BC-GP electrodes exhibited higher voltage efficiency and energy efficiency than pristine graphite, while the voltage efficiency and energy efficiency decreased with increasing of the activation time (AC1 > AC2 > AC3), attributed to the presence of structural disorders of the AC samples.

Sugar cane bagasse is another abundant biowaste material that has been reported for the synthesis of AC. By carbonizing at 700°C with the aid of KOH activation under nitrogen atmosphere, a BET surface area of 1255 m^2 g^{-1} was achieved.[65] The of AC-modified graphene felt electrode showed a reduction in the peak separation (ΔE_p) to 354 mV (vs. 596 mV for thermally treated GF) and higher current at any given potential, as well as nearly 119 times lower charge transfer resistance. The scalability of the VRFB was explored by using a 6-cell stack with 125 cm^2 size electrodes. The AC-modified thermally activated graphene felt was employed as positive electrode. Galvanostatic charge–discharge curves at 100 mA cm^{-2} showed ~76% capacity after 1000 cycles and coulombic, voltage and energy efficiency values of ~83%, 77%, and 64%, respectively.

In another study, domestic fish scales waste was processed into nitrogen self-doped carbon-based nanosheets, using a KOH-assisted hydrothermal approach[66] for their application as negative electrode in VRFBs. The fish scales were processed in 0.01 M KOH, hydrothermally treated, and carbonized at 700 °C in argon (FSC-K). SEM images showed the formation of 2D-nanosheets as a result of the KOH activation step (SEM image shown in **Figure 2**). The elemental composition determined by XPS was C (80.4%), N (5.9%), and O (12.7%). The FSC-K exhibited a BET surface area of 1492 m^2/g, compared to FSC-C, with only 6 m^2/g, demonstrating that the KOH activation treatment is vital to achieve higher, more hydrophilic surface area, due to etching effects and the introduction of oxygen to the surface, which in turn leads to an improvement of the electrocatalytic properties. Electrochemical measurements to explore the electrochemical activity in a three-electrode cell in 1.6 M V^{3+}, 3.0 M H_2SO_4 showed a great electrocatalytic performance of FSC-K towards the V^{2+}/V^{3+} redox pair. The VRFB tests showed that FSC-K deposited onto graphite felt delivered an 18 mA h^{-1} higher discharge capacity (67.2 mA h at 150 mA cm^{-2}), energy efficiency increases by 7.9% (63.8% at 150mAcm^{-2}), and a capacity retention of 83.1% at 75 mAcm^{-2} after 50 cycles, 16.7% larger than pristine carbon felt. The fabrication of the 2D nanosheets through an activation with KOH is an efficient way to enhance the electrochemical performance of carbon electrodes. The basis of this improvement is a combination of increase in surface area via etching, and introduction of N and O functionalities.

Table 1 Decorated carbon felts with biomass-derived carbon for electrocatalysts

Biomaterial	**Activation**	**Carbonization**	**Surface area [m^2/g]**	**Capacity**	**EE**	**Ref.**
Shrimp shell	HTC 200 ℃/ 300 ℃	850 ℃ (N_2)	616 and 102	N/A	N/A	[52]
Pine wood	HTC 200 ℃/ 300 ℃	850 ℃ (N_2)	494 and 436	N/A	N/A	[52]
Sal wood	HTC + $ZnCl_2$ 275 ℃/20 min	850 ℃ (N_2)	1857	N/A	90%	[53]
Orange peel	KOH + 400 ℃ in Ar,	800 ℃ (Ar)	1901	N/A	N/A	[54]
Tea bags	KOH + 600 ℃ in N_2.	800 ℃ (N_2)	2085	31 mA h at 10 mA cm^{-2}	N/A	[55]
Scaphium scaphigerum	Soaked in H_2O +HTC 180℃/ 15 h	$FeCl_3$ + 800 ℃ (Ar)	615.6	81.82 mA h at 100 mA cm^{-2}	69.53%	[56]
Scaphium scaphigerum	Soaked in H_2O + HTC 180 ℃/ 15 h	800 ℃ + K_2FeO_4 (Ar)	1086.9	1599.6 mA h at 50 mA cm^{-2}	72.4%	[57]
Coffee grounds	Hummer's method + reduction to rGO	850 ℃ (N_2)	72	N/A	N/A	[61]
Coffee grounds	Steam-based activation	850 ℃ (N_2)	1113	N/A	N/A	[64]
Sugar cane bagasse	KOH + pre-carbonization 230 ℃/12 h	700 ℃ (N_2)	1255	47 Ah L-1 at 100 mA cm^{-2}	76%	[65]
Fish scales	KOH + HTC 80 ℃ / 24 h	700 ℃ (Ar)	1492	67.2 mA h at 150 mA cm^{-2}	63.8%	[66]

2.2 Strategies to introduce surface functionalities in carbon electrodes

Experimental studies have shown that doping heteroatoms on the surface of carbon electrodes is a very promising method to increase their electrochemical activity in RFBs.[67-69] The number of surface-active sites can be increased by doping, thereby accelerating the adsorption of ions.[70] The difference in electronegativity between carbon and doping atoms (such as N, P, O, S) leads to changes in the electrochemical properties of the carbon electrode.[71, 72] In the previous section, we introduced that dopants are sometimes present in the biomass source and can remain in the resulting carbon. Additionally, a dopant can also be introduced by adding a heteroatom additive during the carbonization process, which results in the introduction of the heteroatom into the forming carbon structure. In fact, the etching reagents presented previously (KOH or K_2FeO_4) are examples to effectively introduce oxygen into the carbon structure. A nitrogen-doped biomass derived activated carbon for RFBs was obtained from kiwi in a one-step activation strategy[73] where the use of ferric ammonium citrate as an active agent led to highly graphitized N-doped porous carbon materials, depicted in **Figure 3**. At high temperatures, ferric ammonium citrate decomposes into Fe-based and NH_3-based materials, introducing N-containing functional groups and contributing to the formation of a porous structure. Kiwi fruits were treated in a hydrothermal process to obtain a carbonaceous hydrogel, which was freeze-dried and then carbonized together with ferric ammonium citrate at 800 °C for 2 hours in argon (named KDC-FAC) and compared to a ferric ammonium citrate-free carbonisation (KDC-C). X-ray diffraction indicated KDC-FAC had the highest graphitisation degree, also confirmed by Raman spectroscopy. XPS was reported a nitrogen content of 2.04 % (vs 1.58% for KDC-C), and a static contact angle for KDC-FAC of 54° (vs. 97°), beneficial for good wettability. The homogeneous doping distribution was confirmed by EDS. CV experiments in 1.6 M V^{3+},3 M H_2SO_4 suggested a superior electrocatalytic activity of KDC-FAC towards V^{2+}/V^{3+} redox pair. A similar trend was reported for the VO^{2+}/VO_2^+ redox pair. EIS measurements suggested that KDC-C and KDC-FAC are controlled by both charge transfer and diffusion processes, with an ohmic resistance (R_s) significantly lower for KDC-FAC caused by a better conductivity and wettability and the smallest charge transfer resistance (R_{ct}), which translated in faster electrochemical kinetics for V^{2+}/V^{3+} redox reaction. KDC-FAC modified carbon felts cell exhibited remarkable electrochemical activity and stability. Compared to pristine electrodes, the energy efficiency improved by 9% at and a capacity retention rate at of 18.24% higher to 55.34%, both at 50 mA cm^{-2}, demonstrating the excellent potential for N-doped AC derived from kiwi as catalyst towards VRFB application. Soaked mature seeds of scaphium scaphigerum were carbonized in the presence of urea to introduce nitrogen in the resulting AC. After hydrothermal treatment, the freeze-dried product was mixed with an excess of urea (4:1 by mass) and carbonized in argon at 850 °C to obtain N-doped AC, with a surface area of 299.42 $m^2\ g^{-1}$.[34] XPS measurements reported a nitrogen content of 8.2%, while carbonising at 700 °C or 1000 °C led to a lower nitrogen content, and a urea free carbonisation at 700 °C resulted in 1.3% nitrogen. CV measurements showed a remarkable increase in current for the N-doped AC and electrochemical activity towards the V^{2+}/V^{3+} redox pair, with a ΔE_p of 141 mV (vs. 451 mV of undoped AC), and the largest oxidation and reduction peak current. Charge-discharge experiments of a single VRFB cell AC modified negative electrode were carried out and compared to pristine electrode. The discharge capacity was 81.5% larger than that of pristine cell (1680.9 mA h vs. 926.3 mA h) at 150 mA cm^{-2} current density. Moreover, the energy efficiency at 150 mA cm^{-2} increased by 9.8% compared with the pristine cell (58.9%). Regarding other reported AC carbon electrodes from the same carbon source (*section 2.1)*, although the overall surface area was significantly lower, the electrocatalytic properties and the overall cell performance showed comparable levels, while greatly improved when compared to pristine electrodes, shown in **Figure 3**.

A similar approach for N-doping was reported by using ammonium oxalate ($(NH_4)_2C_2O_4$) as a nitrogen source and persimmons, an edible fruit, as biomass.[35] The biomass was used to produce a preliminary carbon (PC) via hydrothermal treatment, followed by carbonisation at 750 °C, as schematically shown in **Figure 3**. The PC was then homogenously mixed with ammonium oxalate in different ratios (1:5, 1:10, 1:15), and carbonized again at 750 °C. The BET surface area was reported to increase after the 1:10-ratio carbonization around 2.3 times (16.0 m^2/g from 7.0 m^2/g for PC) due to the etching effect from the decomposing ammonium oxalate. The CV curves indicated that all samples showed catalytic performance towards the VO^{2+}/VO_2^+ reaction, with the 1:10 sample exhibiting the highest current density, a ratio of oxidation peak to reduction peak current density (I_{pa}/I_{pc}) of 2.2 (0.62 lower than that of PC), and peak potential difference of 0.14 V (0.084 V lower than PC). Further investigation and comparison of the catalytic activities were reported through the electrochemical impedance spectra of different samples, proving the lowest R_s and R_{ct} for 1:10 ratio. These results suggested that the treatment with ammonium oxalate can successfully enhance the electrical conductivity. Charge–discharge tests in a VRFB configuration

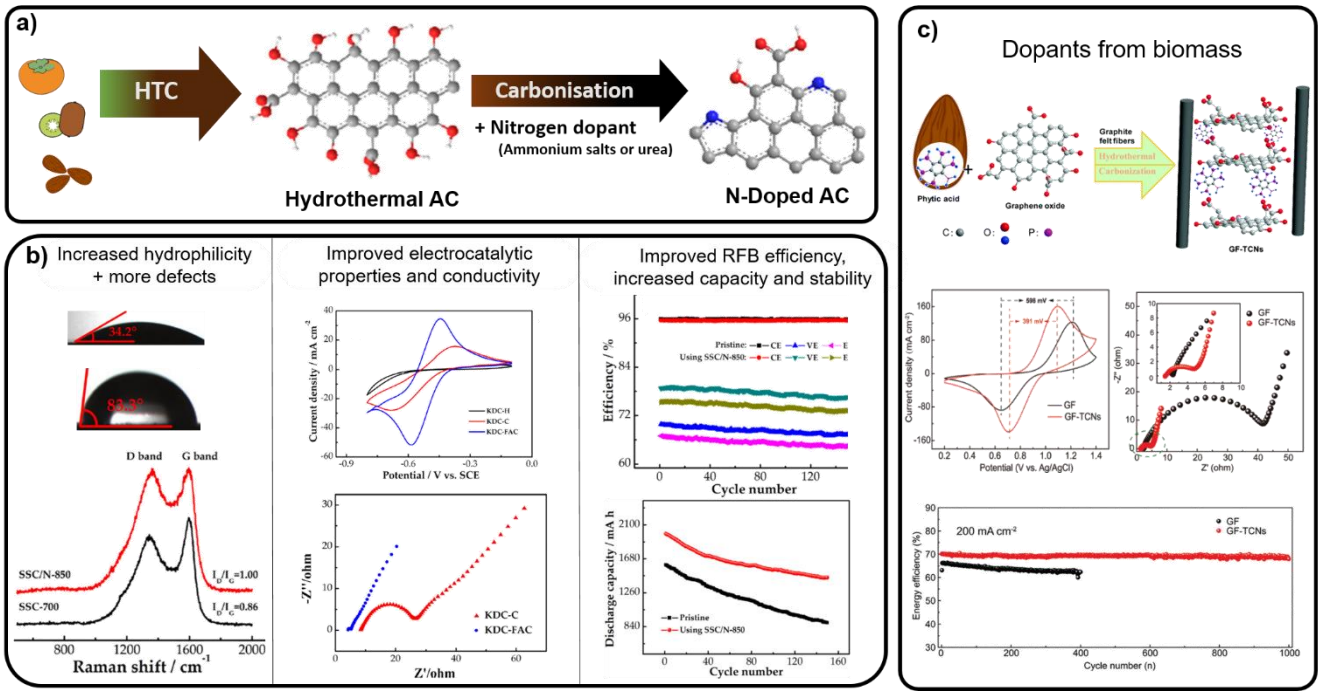

Figure 3 Depiction of the fabrication of doped carbon electrodes for RFB. a) Hydrothermal AC is produced from biomass and ultimately carbonized in the presence of nitrogen containing salts or urea in order to produce N-doped AC. b) N-doped AC shows higher hydrophilicity, due to an insertion of heteroatoms of the carbon structure, as seen in the increasing D-Band in the Raman-spectrum.[35] The resulting electrocatalyc properties of doped AC are characterized as superior to a non-doped comparison by higher activity in CV and lower impedance in EIS. The corresponding RFB with doped AC on carbon felt show as in line of the electrocatalytic effects higher values in capacity, higher performance, as well a higher stability in general. c) An alternative pathway is presented by using a biomass-derived dopant for the modification of rGO.[74] The introduced phosphorous doping shows a similar improving effect as the N-doping of the electrocatalytic properties and a lower impedance. The resulting RFB with P-doped electrodes was reported with an improved and more stable capacity than the corresponding GF without doping.

at 50 mA cm^{-2} for 50 cycles were conducted, revealing a starting discharge capacity of 108.9 mA h, 23.9 mA h higher than the pristine electrode. A higher capacity retention of 89.9% after 50 cycles was reported as well as an EE of 79.9% (vs. 75.9%), proving the treatment with ammonium oxalate is an effective approach to boost the electrocatalytic activity of carbon electrodes.

An alternative strategy is the use of a sustainable sourced dopant that introduces the functional moieties to the electrode. Ling *et al*. reported the cross-linking reaction between phytic acid, a six-fold dihydrogen phosphate ester of inositol, found within the hulls and kernels of seeds, such as almonds, to introduce phosphorus and oxygen functional groups. [74] In combination with reduced graphene oxide (rGO), phytic acid self-assembles into a 3D conductive network *via* the hydrothermal reaction and annealing process. This leads to the formation of a hierarchical electronic and conductive network between the carbon felt for the vanadium ion redox reactions. CV measurements were performed for VO_2^+/VO^{2+} and V^{2+}/V^{3+} redox pairs. The obtained electrodes possessed a higher redox reaction peak current than graphite felt (GF) and a rGO-modified GF, as well as a peak current ratio value (I_{pa}/I_{pc}) closer to 1, and the smallest potential difference ($\Delta E = E_{pa} - E_{pc}$) suggesting higher reversibility and smaller polarization effects. EIS measurements confirmed the new doped electrodes exhibited significantly lower charge transfer resistance. Charge–discharge curves showed a better performance of the doped electrodes, with 27.7% lower initial potential difference, an increase of energy efficiency by 7.0% at 250 mA cm^{-2} and discharge capacity of 10.1 Ah L^{-1} at 350 mA cm^{-2}, while the cell with a GF electrode stopped operating at 300 mA cm^{-2}. The excellent cycling stability of the cell was demonstrated by a steady operation for 1000 cycles at 200 mA cm^{-2} and energy efficiency 70.2%.

Table 2 Chemically doped carbon felts with biomass-derived carbon for electrocatalysts

Carbon Source / Dopant	Activation	Carbonization	Surface area [m^2/g]	Capacity	EE	Ref.
Kiwi / Ferric ammonium citrate	HTC 180 ℃ / 12 h	800 ℃ (Ar) + dopant Ar	N/A	N/A	55.34%	[73]
Scaphium scaphigerum / Urea	Soaked in H_2O + HTC 180 ℃ / 36 h	700/850/1000 ℃ (Ar) +dopant	299.42	1680.9 mA h at 150 mA cm^{-2}	69.7%	[34]
Persimmon / Ammonium oxalate	HTC 140 ℃/10 h.	750 ℃ (Ar) + dopant	N/A	108.9 mA h at 50 mA cm^{-2}	79.9%	[35]
rGO / Phytic acid	HTC + annealing to self-assemble phytic acid + GO onto GF .		N/A	10.1 A h L^{-1} at 350 mA cm^{-2}	N/A	[74]

2.3 Freestanding biomass-derived carbon electrodes

2.3.1 Naturally fibrous biomass-derived carbon electrodes. Even if the use of additional electrocatalytic biomass-derived carbon is a step forward towards the use of more sustainable electrodes, ideally the whole electrode should come from sustainable resources. There have been multiple examples in the literature of biomass-derived carbon electrodes for battery and supercapacitors applications.[13, 75-78] In the case of redox flow batteries, most of the reported research using a purely biomass electrode employ materials that naturally occur as fibers, which then remain fibrous after carbonisation. One example of this are commercial cotton pads.[27] Cotton pads were carbonized at 1000 ˚C in argon, resulting in carbon fibers with a BET surface area of 16.6 m^2 g^{-1}, higher than the comparing thermally treated (6 h at 400 °C in air) commercial carbon paper (OCP) (5.2 m^2/g) or the pristine commercial carbon paper (CP) (1.2 m^2/g). Raman measurements revealed a high degree of graphitization and defects in the carbon structure of the carbonized cotton. This could also be caused by the higher amount of oxygen revealed by XPS, which contributed to a high hydrophilic behaviour. CV measurements in 1 M $VOSO_4$ and 3 M H_2SO_4 showed a potential separation for the carbonized cotton electrode of 180 mV, lower than the OCP electrode (256 mv), as well as higher anodic (I_{pa}) and cathodic peak (I_{pc}) currents of 13.36 mA and 10.57 mA, larger than that for oxidized carbon paper. This was attributed to the larger surface area and the presence of catalytic active sites. When tested in a RFB, the carbonized cotton electrode exhibited lower overpotential and improved charge/discharge than OCP, highlighting the important role of defects and functional groups on the electrocatalytic activity of the carbon electrodes. The VRFB with carbonized cotton electrode presents a discharge capacity of 366 mA h at 100 mA cm^{-2}, > 100 mA h higher than that for oxidized carbon paper. The voltage efficiency (VE) of the RFB with carbonized cotton electrode ranged higher (91% to 75.4%) than that for OCP electrode (from 90% to 68.3%), and more than 10% higher than that of pristine carbon paper. Moreover, pristine carbon paper exhibited particularly poor activity at high current densities. The VRFB with carbonized cotton electrode exhibited the greatest capacity retention, with discharge capacity from 580 mA h to 366 mA h and an energy efficiency (EE) from 87.1% to 74% within the current density range from 40 to 100 mA cm^{-2} as shown in **Figure 4a.** The RFB with oxidized CP only provided 228 mAh at 100 mA cm^{-2}. After changing the current density from 100 to 40 mA cm^{-2}, EE of the battery with carbonized cotton electrode recovered from 74% to 86.3%, higher than that of carbon paper (77.9%) and oxidized carbon paper electrode (84.2%). Overall, the RFB using carbonized cotton electrodes exhibited a great performance, in terms of EE, VE, rate capability and stability. This was due to faster kinetics resulting from the presence of defects and oxygen functional groups at the surface of the electrodes.

Another fibrous biomass derived carbon material that has been reported as freestanding electrode is based on the silk fiber of the bombyx mori cocoon, of which the progression is depicted in **Figure 2b**, a protein-rich natural polymer fiber composite with a nitrogen content of up to 15%, resulting in a nitrogen and oxygen containing carbon electrode.[26] To obtain carbon fibers, the pristine silk fibers were hydrothermally processed

in a 0.06 M Na_2CO_3 solution at 120 °C and carbonized for 4 h at different temperatures (600 °C, 800 °C, or 1000 °C) under argon atmosphere, which was further named as monolithic carbon with enriched nitrogen defects and oxygen groups (NO-MC). As a comparison, pristine CP and OCP, heated 6 h at 500 °C in air, were prepared. The BET surface was much larger for the NO-MC sample (21.16 m^2/g) compared to CP (0.79 m^2/g) and OCP (1.30 m^2/g). Oxygen functional groups were determined by XPS, with ca. 31.05% for NO-MC, higher than CP (ca. 0.00%) and OCP (ca. 24.38%), and a nitrogen content in NO-MC of ca. 5.81%. The graphitic-N content in the samples changed with the carbonization temperature from ca.21.65% for 1000 °C, ca. 19.59% for 800 °C and ca. 17.79% for 600 °C. The influence of the higher amount of oxygen and nitrogen functionalities on the carbon surface could be observed in the contact angle measurements, revealing that CP and OC were both hydrophobic, while the NO-MC exhibits a soaking effect of water, and therefore a contact angle of 0°. CV measurements showed NO-MC electrode led to an improved electrochemical performance for both V^{2+}/V^{3+} and VO^{2+}/VO_2^{+}, with a 50% decrease in redox potential difference and a 192% increase in diffusion slope, compared to commercial carbon paper. This remarkable improvement was attributed to the oxygen functional groups and nitrogen defects. EIS analysis also confirmed the lower charge transfer resistance and the faster mass transfer process. When used as an electrode material in flow batteries, the NO-MC material exhibited a lower charge/discharge overpotential, and higher capacities in comparison with CP and OCP electrodes. The VE for the VRFB with NO-MC electrode decreased from 90% to 75%, with increasing current density from 40 to 100 mA cm^{-2}, less than CP electrode (80% to 63%) and OCP electrode (80% to 69%), proving the better electrochemical reversibility and activity of NO-MC. Furthermore, the average discharge capacity was 83%, a 20% higher energy efficiency than that with CP electrode at the current density of 100 mA cm^{-2}. The NO-MC VRFB also showed the higher stability, strongly suggesting this could be a great candidate for high-performing redox flow battery electrodes.

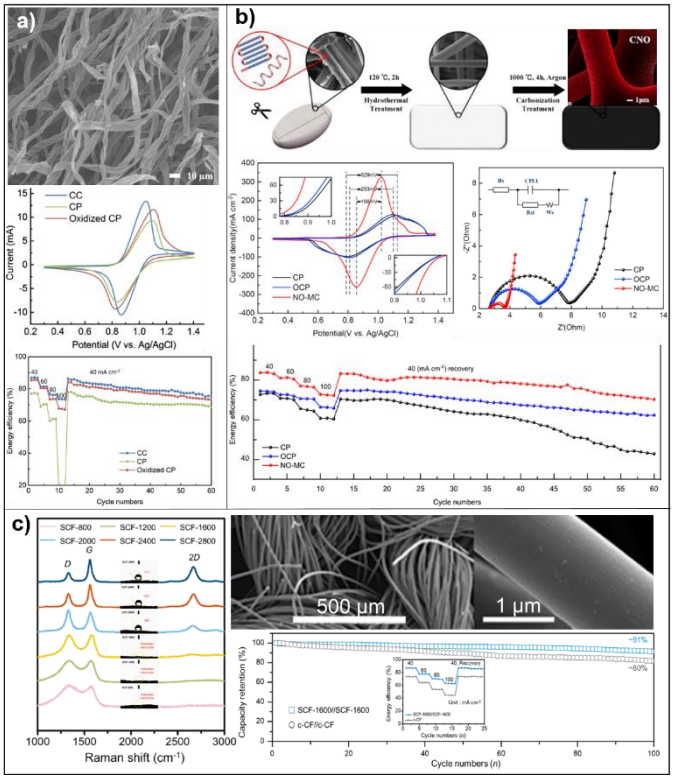

Figure 3 a) Freestanding electrodes made from carbonized cotton (CC) in a direct comparison to CP and OCP. Higher electrocatalytic performance in CV and higher level of defects, resulting into a slightly higher performanec ot the CC after 60 cycles than the OCP, and a significant better performance than the CP.[27] b) Silk derived heteroatom rich electrodes in comparison to CP and OPC. Significant improvement of electrocatalytic properties measured in CV and EIS, as well as for the performance and stability in a RFB.[26] c) Silk derived carbon fibers based on the carbonisation at different temperatures.[25] Increasing graphitisation, shown by Raman measurements, and increasing hydrophobicity was reported for higher temperatures. Hydrophilic carbon fibers from 1600 °C were used for a RFB, resulting in a better stability over 100 cycles (91% capacity retention vs. 80%) higher energt efficienty.

Another report of using silk protein-derived carbon fabrics was reported be Lee et. al.[25] In this report, commercial silk was used to isolate the containing protein and resulting in heteroatom rich carbon fibers after carbonization. Subsequent heating between 1200 °C and 2800 °C under argon atmosphere was reported to obtain silk protein-derived carbon fabrics (SCF), which all maintaining their fabric shapes with average diameters about 10 µm. The comparing data of the different resulting carbon fibers from different temperatures are depicted in an overview in **Figure 4c**. The surface areas were decreasing with increasing temperature in the range of 5.1 m^2/g at 800 °C (SCF-800) and 3.0 m^2/g for SCF-2800. XPS was reported with an increase of carbon content from 64.1% (O = 20.4%; N = 15.5%) for SCF-800 to 97.2% (O = 1.5%; N = 1.3%) for SCF-2800. Raman spectroscopy

measurement confirmed a D and G band ratio (I_D/I_G) decrease with increasing (range from 2.10 for SCF-800 down to 0.48 for SCF- 2800), as shown in **Figure 4c** together with the CV-changes in dependence of carbonization temperature. In addition to that, the in-plane crystallite size of SCFs (L_a) were reported with increasing size (2.1 nm SCF-800 up to 9.2 nm for SCF- 2800) and in addition, SCF-2000 and temperature wise upwards a well-defined 2D band centred at 2,670 cm^{-1} is visible, which is due to the presence of stacked graphitic layers, which was confirmed by XRD and TEM.[25, 79, 80] Compared to a commercial carbon felt electrode with a comparable oxygen content (C/O ratio = 12.4) to SCF-1600 (13.2), the ΔE_p in the CV (for commercial carbon felt: 434.2 mV and 363.5 mV; SCF-1600 164.5 mV, 186.4 mV in catholyte and anolyte, respectively) were considerably lower for the SCF-1600, which was attributed to the enhancing effect of the high electron density of pyridinic-N structure in the electron transfer kinetics for vanadium redox reactions.

The electrocatalytic activity was supported by EIS analysis. Both redox reactions showed lower charge transfer resistance for the SCF-1600 electrode compared with that of commercial CF electrode. VRFBs were assembled using SCF-1600, as well as a cell with commercial carbon felt electrodes for comparison. The SCF-1600 electrodes exhibited higher specific capacity of 32.5 Ah L^{-1} (vs. 22.2 Ah L^{-1}, both measured between 0.8–1.6 V at 40 mA cm^{-2}), a voltage efficiency of 61.1% (100 mA cm^{-2}, 45.1% higher than commercial carbon felt electrodes). Energy efficiency value of 86.8% was obtained at 40 mA cm^{-2} for the SCF-1600 electrodes, with capacity retention after 100 cycles of 91%, compared to 80% observed for commercial carbon felt electrodes, demonstrating the great potential of the SCF-1600 electrodes.

2.3.2 Processing of biomass materials into fibers by electrospinning.

Electrospinning is a well-known technique for the fabrication of submicron- and nanosized polymer fibers from a polymer solution or a melt. In electrospinning, electrostatic forces are used to charge the formed droplet of a solution at the tip of the metallic needle of a syringe, causing the formation of a Taylor-cone towards a grounded collector. A schematic depiction of a standard electrospinning process is shown in **Figure 5b**. The physical entanglement of the polymer prevents a breaking of the thinning Taylor-cone, leading to the formation fibers while the solvent fully evaporates or the melt freezes.[81-83] PAN has been reported to be very suitable for electrospinning and an excellent method to create carbon nanofibers for a variety of applications[84], including supercapacitors [85, 86], lithium-ion batteries [87-90], or redox flow batteries.[91-93] The fabrication of biomass derived electrospun carbon nanofibers has been increasingly explored in the last decade due to the versatility of the method. Notable biomass-derived alternatives for the formation of carbon fibers are based on the electrospinning of lignin[94-96], cellulose [97, 98], or chitosan.[90] The utilization in RFBs remains a relatively new and undiscovered field.

Lignin, one of the most abundant biopolymers, offers a range of advantages that make it suitable candidate, including low-cost, high aromatic carbon content, or a variety of functional oxygen containing groups, in addition to a good suitability for electrospinning.[99] More than 60 megatons per year are produced as by-product of the cellulose pulping process and predominantly used as low-value waste products and mainly been burned for heat and power generation, as it possesses high calorific value.[100] While high value utilisations of lignin are still limited, the potential of lignin in industrial applications are gaining more attention because of its aromatic structure and the sustainability of the material itself[101], as well as other properties, such as chemical and thermal stability and biodegradability.[99] All these properties make lignin of great interest for practical applications.[102] For the past few years, lignin and its derivatives have been reported to be used in energy storage applications as binders[103], electrolyte additives[104], membranes[105], and promising electrode materials.[106, 107] Compared to other electrode materials, the use of lignin in energy storage devices improves sustainability while remaining at high performance and graphitisation, contributing to the development of more sustainable energy storage devices.

In particular, lignin-derived carbon nanofibers (CNFs) are a promising candidate as alternative material for RFB electrodes. The structure and composition of the electrode will affect the overpotential which directly impacts the performance of the battery, in terms of voltage efficiency. Therefore, the study of the structure-property relationship in these systems is key to achieve high performing sustainable electrodes. Since lignin is a biopolymer, the source has great influence in the material properties, but overall lignin consists of the same main monomeric units, shown in **Figure 5a**. Paracoumaryl alcohol (1), coniferyl alcohol (2) and sinapyl alcohol (3), which then form a complex structured phenolic macromolecule, which considerably varies with dependence on the source and the isolation process.[108] Vivo-Vilches *et al.* reported in 2019 the electrospinning of three different types of lignin (kraft lignin (KL), ethanol organosolv lignin and phosphoric acid lignin (PL)) as precursors in combination with polyethylene oxide (PEO) as plasticiser, and the electrochemical properties of the lignin-derived carbon fibers for the vanadium redox couples. The solutions consist of lignin/PEO ratio (90/10, 20 wt.% in DMF). Additionally, a

solution was spun with addition 1 wt.% conductive carbon to improve electrochemical performance of the deriving carbon fibers. The electrospun mats were either preheated in air to 200 °C or directly carbonized to obtain CNFs, except for ethanol organosolv lignin originated fibers, since the fibrous structure was lost the treatment and poor mechanical properties and shrinkage induced by carbonization made testing in electrochemistry impossible according to the author.

The CNFs deriving from PL and KL showed identical I_D/I_G in Raman spectroscopy (0.88), while the percentage of heteroatom in PL (O = 11.7wt.% P = 1.2 wt.%) was lower than in KF (O= 16.2 wt.%). Fibers from KL with additional conductive carbon were reported with 9.1 wt% oxygen. The use of different voltages led to different fiber diameter for KF resulting in diameters of 226 ± 22 nm (7 kV) and 215 ± 33 nm (9 kV). A scanning electron microscopy (SEM) image of the fibers with the lowest diameter is shown in **Figure 5c**. In a direct comparison of the electrochemical properties via CV (solution of 0.15 M V^{3+}/V^{4+} stoichiometric mixture in 3 M H_2SO_4) PL-derived CNFs show the peaks are more intense for the oxidation and reduction of vanadium species than that of the KL-derived CNF. The oxidation and reduction potentials were yet very similar in the two cases, giving peak potential differences ΔE_p = 0.6 V for V^{5+}/V^{4+} and ΔE_p = 0.3 V for V^{3+}/V^{2+}. Adding conductive carbon during the electrospinning process of KL Increased the activity for vanadium electrochemistry with an increase of the intensity of the signals related to vanadium species reduction and oxidation and reduced the potential differences between oxidation and reduction ΔE_p = 0.4 V for V^{5+}/V^{4+} and ΔE_p = 0.2 V for V^{3+}/V^{2+}. This work demonstrated the successful application of electrospun lignin-derived carbon electrodes for vanadium-based electrochemistry and potentially a lignin-derived alternative with improved properties for existing VRFB systems.

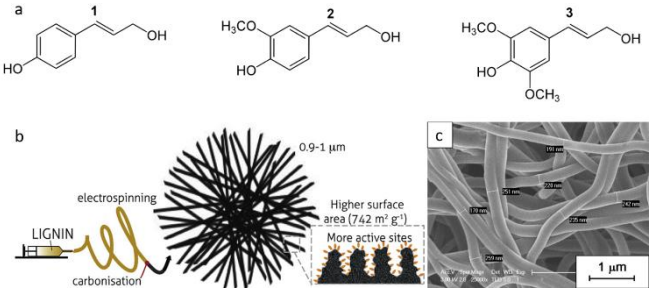

Figure 4 a) Main monomer units of lignin: Paracoumaryl alcohol (1), coniferyl alcohol (2) and sinapyl alcohol (3) which make up the polymer network to form lignin. b) Schematic depiction the fabrication of electro spun carbon fibers (diameter 0.9-1.0 µm, 742 m^2/g) for electrodes in VRFBs with outstanding high surface-to-volume ratio.[110] c) SEM image of the electrospun fibers from a mixture of kraft lignin (90 wt.%) and PEO. The fibers were obtained with an average diameter of 215 ± 33 nm.[104]

A full report on the use of lignin derived CNFs used a different strategy to from a suitable solution for the electrospinning process was reported of using a high molecular lignin fraction instead of blending lignin a high molecular polymer. Softwood kraft lignin was obtained from a LignoBoost process,[109] and then fractionated with by successive extraction with organic solvents [110] to obtain a higher molecular weight fraction of lignin, which then could be electrospun in DMF to result in fibers from pure lignin that have a diameter of ~750-1000 nm.[111] The obtained CNFs were prepared by preheating the fibrous mat at 250 °C for 30 min and then carbonized at 800 °C for 2 hours. To introduce a P-doping, the CNFs were soaked in a 2 M solution of ammonium hexafluorophosphate, dried and annealed at 2 h at 500 °C. A commercial non-woven carbon fiber fabric sheet was used comparison and treated with the same procedure. The BET surface area for pristine CNFs was reported to be around 14 times higher (742 vs. 41m^2/g), which allows the exposure of more active sites, as depicted in **Figure 6b**, together with a schematic electrospinning setup. A decrease in BET surface area of the CNF electrode was observed after P-doping to a value of 27 m^2/g, which is attributed to micro and mesopore blockage s. Spectroscopic measurements revealed a higher content of oxygen-containing groups for the initial CNF material (9.21 vs. 1.9 at.%) in XPS, and a higher proportion of defects for the with a ratio of I_D/I_G (1.17 vs 1.02). After the doping process of both fiber mats, a higher P-content (2.8 vs. 0.18 at.%) and N-content (2.91 vs 0.99 at.%) was reported for the electrospun CNFs, and an overall decrease of the measured defects in Raman spectroscopy to 1.08 for the CNFs vs. 1.01 for the commercial carbon fiber fabric.

For the electrocatalytic activity towards the redox reactions of vanadium (V^{3+}/V^{2+} and VO_2^+/VO^{2+}) in CV measurements, the pristine CNF sample was reported to perform significantly better than the commercial fiber mat, as cathodic and anodic current densities. P-doping on the commercial fibers favours the VO^{2+}/VO_2^+ reaction by increasing the peaks intensity. . Surprisingly, the introduction of P in the CNF samples resulted counterproductive, with a decrease in electrochemical performance, attributed to a reduction of active sites due to steric hindrance of phosphate groups and decrease in BET surface area. The electrical conductivity was reported to be significantly lower for the CNFs (9.8 vs. 25.3 S/m) and the doped CNF (2.6 vs. 19.6 S/m) compared to the commercial fiber sheet. Despite having much lower conductivity values the pristine electrospun material is on a comparable to that observed for the commercial fiber sheet, suggesting that improvements to and optimization of the electrospinning, carbonization, and doping process could mean lignin-based

carbon materials are performance to commercial standard, while originating from fully sustainable source. of lignin-derived electrospun CNF mat as alternative sustainable electrodes for VRFB. Electrochemical characterization demonstrated a higher electrochemical activity towards the VO^{2+}/VO_2^+ reaction for the lignin-derived CNFs compared with commercial felts, attributed to the higher surface area and higher amount of oxygen functional groups. In addition, the RFB with lignin-derived electrodes exhibited comparable performance to commercial carbon.

3. Summary

Redox flow batteries are promising large-scale energy storage devices which have drawn significant attention in the last decade, due to their scalability, flexibility and low-cost. Further improvements in reliability and power output of redox flow battery strongly rely on the structural and electrochemical properties of the electrodes. Among the contenders, carbon composites have been studied for most energy technologies, including redox flow battery electrodes. Lately, the research in sustainable resources, and in particular, biomass-derived carbon electrode materials have experienced great interest, with the number of publications in this topic raising quickly in the last few years, a step forward towards the independence from petrol-derived materials. The use of biomass-derived carbon materials for energy storage devices has been focused of interest for a few years now, particularly in supercapacitors and ion-batteries. However, only recently biomass materials have been studied for redox flow batteries, perhaps also attributed to the increasing interest in alternative grid-scale and stationary energy storage technologies.

Recent reported works on biomass-derived carbon show how electrodes can be made from or improved by virtually any given biomass and has been demonstrated to be a simple and efficient approach to increase the electrochemical active surface area by using it in addition to an existing carbon felt. The choice of biomaterial allows to influence the chemical composition of the derived carbon electrode material and achieve doping with relevant chemical elements or functional groups that can drastically enhance the electrocatalytic performance of the electrodes. Using additives during the carbonization step enables the increase in surface area, and hence a higher number of reactions can take place. It is also another strategy that can lead to the introduction of heteroatoms such as N, S, or P and further improve the electrocatalytic properties of the carbon electrodes by lowering the peak potential difference and reaching peak current ratio value closer to 1. All-biomass derived electrodes constitute the ultimate approach to produce sustainable carbon electrodes. Naturally fibrous biomass structures have showed excellent performance for RFB electrode applications. In addition, preliminary works using electrospinning to create freestanding carbon fiber electrodes have showed great promise. Overall, the variety different biomass precursors and strategies discussed here showcase the great potential of biomass-derived carbons as the next generation of electrode materials for redox flow batteries.

4. Future outlook

Redox flow batteries have the potential to become the future of stationary energy storage. The electrocatalytic properties of the electrodes enhanced by biomass-derived have proven to be far better than pristine commercial carbons, which need to undergo an energy intense post-treatment to become functional electrode materials. The addition of biomass derived carbons is an efficient way to improve the properties of the existing commercial carbon fibers. Particularly, electrospinning offers a flexible way to process biomass into freestanding materials that has been implemented in the design of electrodes for supercapacitors and metal-ion batteries. Long-term stability and cost efficiency are important parameters for large-scale energy storage applications that needs improving in biomass-derived materials. Ideally, the sustainable carbon source would come from local biowaste. In fact, some of the examples shown in this review can be found locally almost everywhere include spent coffee grounds, used tea bags, and lignin, which then need to be available in a suitable amount to cover the demand. Self-doping, additive doping, and etching are some of the strategies that have been proposed to improve electrocatalytic performance of carbon electrodes. However, more in-depth research into the individual effect of each approach is needed. Introduction of abundant electrocatalytic metals, such as Fe or Mn, and their oxides, have not yet been reported for biomass-derived RFB electrodes. The potential of these metal catalyst has been explored for PAN-derived carbon remarkable electrochemical performance.[112-114] Especially the combination of electrospinning of biomaterials for the fabrication of carbon fiber in micro- and nanometre dimensions has a high potential for the fabrication a fully sustainable electrode. The versatility of this method also allows a large variation to adapt to the given biomaterials and include the catalyst into the electrospun fiber. The flexibility of these methods will be an important factor when alternative redox flow batteries will emerge, and there a variation of the pore size and surface properties will most likely be needed. Especially RFB with organic or polymeric redox species have become more popular over the recent years and are likely to become a valid alternative to vanadium, due to its high price and the large

amount needed in order to build large scale energy storage. Finally, the porous channels and interconnectivity of the porosity of the electrospun carbon electrodes will also be key in order to optimize the performance of the biomass-derived carbon fibers and more research should be conducted in this area to combine electrocatalytic effect with electrolyte fluid dynamics through the electrode and the whole device.

Table 3 Freestanding carbon fibers from biomass-derived carbon

Carbon fiber source	**Activation Heteroatoms**	**Carbonization**	**Surface area [m^2/g]**	**Capacity**	**EE**	**Ref.**
Cotton	N/A	1000 °C (Ar)	16.6	N/A	N/A	[27]
Silk fibers	Hydrothermal 120 °C/2 h	600/800/1000 °C (Ar)	21.16, 0.79, and 1.30	580 mA h to 366 mA h, 40 to 100 mA cm^{-2}	87.1% to 74% from 40 to 100 mA cm^{-2}	[26]
Silk protein fibers	Heated to 800 °C (N_2)	1200-2800°C (Ar)	3.0 - 5.1	32.5 Ah L^{-1} at 40 mA cm^{-2}	~86.8%	[25]
Electrospun lignin/PEO (9/1) + carbon	Heated to 200 °C (Air)	1000 °C (N_2)	N/A	N/A	N/A	[108]
Electrospun lignin	Heated to 250 °C (Air)	800 °C (N_2)	742	~670 mA h ~ at 40 mA cm^{-2}	~ 79%	[111]
Electrospun lignin + Ammonium hexafluorophosphate	Heated to 250 °C (Air)	800 °C (N_2) + 500 °C with dopant	27	~630 mA h ~ at 40 mA cm^{-2}	~ 78%	[111]

Acknowledgements

AJS acknowledges her UKRI Future Leaders Fellowship (MR/T041412/1) for their support. GT acknowledges the Chinese Studentship Council for supporting his PhD.

References

[1] Masson-Delmotte V, P. Zhai, A. Pirani, S.L. Connors, C. Péan, S. Berger, N. Caud, Y. Chen, L. Goldfarb, M.I. Gomis, M. Huang, K. Leitzell, E. Lonnoy, J.B.R. Matthews, T.K. Maycock, T. Waterfield, O. Yelekçi, R. Yu,and B. Zhou (eds.) 2021 *Cambridge University Press*

[2] Dinesh A, Olivera S, Venkatesh K, Santosh M S, Priya M G, Inamuddin, Asiri A M and Muralidhara H B 2018 *Environmental Chemistry Letters* **16** 683

[3] Thaller L H 1974 *9th Intersociety Energy Conversion Engineering Conference* 924

[4] Khor A, Leung P, Mohamed M R, Flox C, Xu Q, An L, Wills R G A, Morante J R and Shah A A 2018 *Materials Today Energy* **8** 80

[5] Yuan Z, Yin Y, Xie C, Zhang H, Yao Y and Li X 2019 *Adv Mater* **31** 1902025

[6] Li B, Nie Z, Vijayakumar M, Li G, Liu J, Sprenkle V and Wang W 2015 *Nat Commun* **6** 1

[7] Houser J, Clement J, Pezeshki A and Mench M M 2016 *Journal of Power Sources* **302** 369

[8] Zhang H, Tan Y, Li J and Xue B 2017 *Electrochimica Acta* **248** 603

[9] Lin C H, Zhuang Y D, Tsai D G, Wei H J and Liu T Y 2020 *Polymers (Basel)* **12** 1372

[10] Pezeshki A M, Clement J T, Veith G M, Zawodzinski T A and Mench M M 2015 *Journal of Power Sources* **294** 333

[11] Dixon D, Babu D J, Langner J, Bruns M, Pfaffmann L, Bhaskar A, Schneider J J, Scheiba F and Ehrenberg H 2016 *Journal of Power Sources* **332** 240

[12] Hassan A and Tzedakis T 2019 *Journal of Energy Storage* **26** 100967

[13] Liu J, Yuan H, Tao X, Liang Y, Yang S J, Huang J Q, Yuan T Q, Titirici M M and Zhang Q 2020 *EcoMat* **2** e12019

[14] Wu X, Xu H, Shen Y, Xu P, Lu L, Fu J and Zhao H 2014 *Electrochimica Acta* **138** 264

[15] Zhang W, Xi J, Li Z, Zhou H, Liu L, Wu Z and Qiu X 2013 *Electrochimica Acta* **89** 429

[16] Lourenssen K, Williams J, Ahmadpour F, Clemmer R and Tasnim S 2019 *Journal of Energy Storage* **25** 100844

[17] Asaadi S, Hummel M, Hellsten S, Harkasalmi T, Ma Y, Michud A and Sixta H 2016 *ChemSusChem* **9**

[18] Hauru L K J, Hummel M, Michud A and Sixta H 2014 *Cellulose* **21** 4471

[19] Choi J, Zequine C, Bhoyate S, Lin W, Li X, Kahol P and Gupta R 2019 *C* **5** 44

[20] Zhao X, Li C, Zhang X, Sun X, Wang K, Huang X and Ma Y 2017 *ChemistrySelect* **2** 6194

[21] Yan J 2020 *International Journal of Electrochemical Science* **15** 1982

[22] Wang Q, Li Y, Wang K, Zhou J, Zhu L, Gu L, Hu J and Cao X 2017 *Electrochimica Acta* **257** 250

[23] Zhao G, Li Y, Zhu G, Shi J, Lu T and Pan L 2019 *ACS Sustainable Chemistry & Engineering* **7** 12052

[24] Gao S, Li L, Geng K, Wei X and Zhang S 2015 *Nano Energy* **16** 408

[25] Lee M E, Jang D, Lee S, Yoo J, Choi J, Jin H-J, Lee S and Cho S Y 2021 *Applied Surface Science* **567** 150810

[26] Wang R and Li Y 2019 *Journal of Power Sources* **421** 139

[27] Zhang Z H, Zhao T S, Bai B F, Zeng L and Wei L 2017 *Electrochimica Acta* **248** 197

[28] Dennison C R, Agar E, Akuzum B and Kumbur E C 2015 *Journal of The Electrochemical Society* **163** A5163

[29] Zhou X L, Zhao T S, An L, Zeng Y K and Wei L 2017 *Journal of Power Sources* **339** 1

[30] Bi Z, Kong Q, Cao Y, Sun G, Su F, Wei X, Li X, Ahmad A, Xie L and Chen C-M 2019 *Journal of Materials Chemistry A* **7** 16028

[31] Dos Reis G S, Larsson S H, de Oliveira H P, Thyrel M and Claudio Lima E 2020 *Nanomaterials (Basel)* **10** 1398

[32] Culebras M, Geaney H, Beaucamp A, Upadhyaya P, Dalton E, Ryan K M and Collins M N 2019 *ChemSusChem* **12** 4516

[33] Eifert L, Banerjee R, Jusys Z and Zeis R 2018 *Journal of The Electrochemical Society* **165** A2577

[34] Jiang Y, Du M, Cheng G, Gao P, Dong T, Zhou J, Feng X, He Z, Li Y, Dai L, Meng W and Wang L 2021 *Journal of Energy Chemistry* **59** 706

[35] Zhang T, Zhu Y, Lv Y, Yu Q, Yao S, Zhu W and He Z 2021 *Ionics* **27** 4771

[36] Yang H, Fan C and Zhu Q 2017 *Journal of Electrochemical Energy Conversion and Storage* **14** 041004

[37] Hirokazu Ishitobi S S, Kosuke Oba, Nobuyoshi Nakagawa 2020 *Advanced Engineering Forum* **38** 31

[38] Jiang F, He Z, Guo D and Zhou X 2019 *Journal of Power Sources* **440** 227114

[39] Yang Y, Ma W, Zhang T, Ye D, Chen R and Zhu X 2020 *Chem Commun (Camb)* **56** 14984

[40] González Z, Flox C, Blanco C, Granda M, Morante J R, Menéndez R and Santamaría R 2017 *Journal of Power Sources* **338** 155

[41] Gürsu H, Gençten M and Şahin Y 2018 *Ionics* **24** 3641

[42] Hu G, Jing M, Wang D-W, Sun Z, Xu C, Ren W, Cheng H-M, Yan C, Fan X and Li F 2018 *Energy Storage Materials* **13** 66

[43] Sankar A, Michos I, Dutta I, Dong J and Angelopoulos A P 2018 *Journal of Power Sources* **387** 91

[44] Deng Q, Huang P, Zhou W-X, Ma Q, Zhou N, Xie H, Ling W, Zhou C-J, Yin Y-X, Wu X-W, Lu X-Y and Guo Y-G 2017 *Advanced Energy Materials* **7** 1700461

[45] Nia P M, Abouzari-Lotf E, Woi P M, Alias Y, Ting T M, Ahmad A and Che Jusoh N W 2019 *Electrochimica Acta* **297** 31

[46] Etienne M, Vivo-Vilches J F, Vakulko I, Genois C, Liu L, Perdicakis M, Hempelmann R and Walcarius A 2019 *Electrochimica Acta* **313** 131

[47] Li Q, Bai A, Qu Z, Zhang T, Li J, Zhang X, Yu M, Xue Z and Sun H 2019 *Journal of Chemistry* **2019** 1

[48] Zhao C, Li Y, He Z, Jiang Y, Li L, Jiang F, Zhou H, Zhu J, Meng W, Wang L and Dai L 2019 *Journal of Energy Chemistry* **29** 103

[49] Aziz M A, Hossain S I and Shanmugam S 2020 *Journal of Power Sources* **445** 227329

[50] Radford G J W, Cox J, Wills R G A and Walsh F C 2008 *Journal of Power Sources* **185** 1499

[51] Zhou H, Zhang H, Zhao P and Yi B 2006 *Electrochimica Acta* **51** 6304

[52] Wan C T-C, López Barreiro D, Forner-Cuenca A, Barotta J-W, Hawker M J, Han G, Loh H-C, Masic A, Kaplan D L, Chiang Y-M, Brushett F R, Martin-Martinez F J and Buehler M J 2020 *ACS Sustainable Chemistry & Engineering* **8** 9472

[53] Maharjan M, Wai N, Veksha A, Giannis A, Lim T M and Lisak G 2019 *Journal of Electroanalytical Chemistry* **834** 94

[54] Maharjan M, Bhattarai A, Ulaganathan M, Wai N, Oo M O, Wang J-Y and Lim T M 2017 *Journal of Power Sources* **362** 50

[55] Abbas A, Abbas S, Bhattarai A, Latiff N M, Wai N, Phan A N and Lim T M 2021 *Journal of Power Sources* **488** 229411

[56] Jiang Y, Cheng G, He Z, Chen J, Li Y, Zhu J, Meng W, Zhou H, Dai L and Wang L 2019 *Journal of The Electrochemical Society* **166** A3918

[57] Lv Y, Li Y, Han C, Chen J, He Z, Zhu J, Dai L, Meng W and Wang L 2020 *J Colloid Interface Sci* **566** 434

[58] Andrade T S, Vakros J, Mantzavinos D and Lianos P 2020 *Chemical Engineering Journal Advances* **4** 100061

[59] Kim H-J and Oh S-C 2021 *Applied Sciences* **11** 6542

[60] Kovalcik A, Obruca S and Marova I 2018 *Food and Bioproducts Processing* **110** 104

[61] Abbas A, Eng X E, Ee N, Saleem F, Wu D, Chen W, Handayani M, Tabish T A, Wai N and Lim T M 2021 *Journal of Energy Storage* **41** 102848

[62] Handayani M, Ganta M, Susilo D N A, Yahya M S, Sunnardianto G K, Darsono N. Sulistiyono E, Setiawan I, Lestari F P and Erryani A 2019 *IOP Conf. Series: Materials Science and Engineering* **541** 012032

[63] Park S, An J, Potts J R, Velamakanni A, Murali S and Ruoff R S 2011 *Carbon* **49** 3019

[64] Krikstolaityte V, Joshua O, Veksha A, Wai N, Lisak G and Lim T 2018 *Batteries* **4** 56

[65] Mahanta V, Raja M and Kothandaraman R 2019 *Materials Letters* **247** 63

[66] He Z, Cheng G, Jiang Y, Li Y, Zhu J, Meng W, Zhou H, Dai L and Wang L 2020 *International Journal of Hydrogen Energy* **45** 3959

[67] Fu S, Zhu C, Song J, Engelhard M H, Du D and Lin Y 2017 *Electroanalysis* **29** 1469

[68] Huang Y, Deng Q, Wu X and Wang S 2017 *International Journal of Hydrogen Energy* **42** 7177

[69] Yang D-S, Lee J Y, Jo S-W, Yoon S J, Kim T-H and Hong Y T 2018 *International Journal of Hydrogen Energy* **43** 1516

[70] Wang S, Zhao X, Cochell T and Manthiram A 2012 *J Phys Chem Lett* **3** 2164

[71] Jiang H R, Shyy W, Zeng L, Zhang R H and Zhao T S 2018 *Journal of Materials Chemistry A* **6** 13244

[72] Schnucklake M, Eifert L, Schneider J, Zeis R and Roth C 2019 *Beilstein J Nanotechnol* **10** 1131

[73] Cheng D, Tian M, Wang B, Zhang J, Chen J, Feng X, He Z, Dai L and Wang L 2020 *J Colloid Interface Sci* **572** 216

[74] Ling W, Wang Z A, Ma Q, Deng Q, Tang J F, Deng L, Zhu L H, Wu X W, Yue J P and Guo Y G 2019 *Chem Commun (Camb)* **55** 11515

[75] Gong Y, Li D, Luo C, Fu Q and Pan C 2017 *Green Chemistry* **19** 4132

[76] Lu H and Zhao X S 2017 *Sustainable Energy & Fuels* **1** 1265

[77] Reis G S D, Oliveira H P, Larsson S H, Thyrel M and Claudio Lima E 2021 *Nanomaterials (Basel)* **11** 424

[78] Wang Y, Qu Q, Gao S, Tang G, Liu K, He S and Huang C 2019 *Carbon* **155** 706

[79] Cho S Y, Yun Y S, Lee S, Jang D, Park K Y, Kim J K, Kim B H, Kang K, Kaplan D L and Jin H J 2015 *Nat Commun* **6** 7145

[80] Choi J, Lee M E, Lee S, Jin H-J and Yun Y S 2019 *ACS Applied Energy Materials* **2** 1185

[81] Greiner A and Wendorff J H 2007 *Angew Chem Int Ed Engl* **46** 5670

[82] Ibrahim Y S, Hussein E A, Zagho M M, Abdo G G and Elzatahry A A 2019 *Int J Mol Sci* **20** 2455

[83] Teo W E and Ramakrishna S 2006 *Nanotechnology* **17** 89

[84] Yadav D, Amini F and Ehrmann A 2020 *European Polymer Journal* **138** 109963

[85] Liang J, Zhao H, Yue L, Fan G, Li T, Lu S, Chen G, Gao S, Asiri Abdullah M and Sun X 2020 *Journal of Materials Chemistry A* **8** 16747

[86] Lu X, Wang C, Favier F and Pinna N 2017 *Advanced Energy Materials* **7** 1601301

[87] Duan B, Gao X, Yao X, Fang Y, Huang L, Zhou J and Zhang L 2016 *Nano Energy* **27** 482

[88] Javed K, Oolo M, Savest N and Krumme A 2018 *Critical Reviews in Solid State and Materials Sciences* **44** 427
[89] Nowak A P, Hagberg J, Leijonmarck S, Schweinebarth H, Baker D, Uhlin A, Tomani P and Lindbergh G 2018 *Holzforschung* **72** 81
[90] Wang Z, Kang K, Wu J, Hu Q, Harper D P, Du G, Wang S and Xu K 2021 *Journal of Materials Research and Technology* **11** 50
[91] Cheng D, Li Y, Zhang J, Tian M, Wang B, He Z, Dai L and Wang L 2020 *Carbon* **170** 527
[92] Liu S, Kok M, Kim Y, Barton J L, Brushett F R and Gostick J 2017 *Journal of The Electrochemical Society* **164** A2038
[93] Schnucklake M, Cheng M, Maleki M and Roth C 2021 *Journal of Physics: Materials* **4** 032007
[94] Adam A A, Ojur Dennis J, Al-Hadeethi Y, Mkawi E M, Abubakar Abdulkadir B, Usman F, Mudassir Hassan Y, Wadi I A and Sani M 2020 *Polymers (Basel)* **12** 2884
[95] García-Mateos F J, Ruiz-Rosas R, María Rosas J, Morallón E, Cazorla-Amorós D, Rodríguez-Mirasol J and Cordero T 2020 *Separation and Purification Technology* **241** 116724
[96] Li Z, Liu J, Jiang K and Thundat T 2016 *Nano Energy* **25** 161
[97] Deng L, Young R J, Kinloch I A, Abdelkader A M, Holmes S M, De Haro-Del Rio D A and Eichhorn S J 2013 *ACS Appl Mater Interfaces* **5** 9983
[98] Yang C, Chen C, Pan Y, Li S, Wang F, Li J, Li N, Li X, Zhang Y and Li D 2015 *Electrochimica Acta* **182** 264
[99] Svinterikos E, Zuburtikudis I and Al-Marzouqi M 2020 *ACS Sustainable Chemistry & Engineering* **8** 13868
[100] Rodríguez J J, Cordero T and Rodríguez-Mirasol J 2016 *Production of Biofuels and Chemicals from Lignin*, **8** 217
[101] Yoo C G and Ragauskas A J 2021 *From Processing to Applications.* **1** 1
[102] Bajwa D S, Pourhashem G, Ullah A H and Bajwa S G 2019 *Industrial Crops and Products* **139** 111526
[103] Lu H, Cornell A, Alvarado F, Behm M, Leijonmarck S, Li J, Tomani P and Lindbergh G 2016 *Materials (Basel)* **9** 127
[104] Liu B, Huang Y, Cao H, Song A, Lin Y, Wang M and Li X 2017 *Journal of Solid State Electrochemistry* **22** 807
[105] Ye J, Lou X, Wu C, Wu S, Ding M, Sun L and Jia C 2018 *Front Chem* **6** 549
[106] Liu H, Xu T, Liu K, Zhang M, Liu W, Li H, Du H and Si C 2021 *Industrial Crops and Products* **165** 113425
[107] Roman J, Neri W, Derré A and Poulin P 2019 *Carbon* **145** 556
[108] Vivo-Vilches J F, Celzard A, Fierro V, Devin-Ziegler I, Brosse N, Dufour A and Etienne M 2019 *Nanomaterials (Basel)* **9** 106
[109] Tomani P 2010 *Cellulose Chem. Technol.* **44** 53
[110] Moerck R Y, H.; Kringstad, K.P.; Hatakeyama, H. 1987 *Holzforschung* **40** 51
[111] Ribadeneyra M C, Grogan L, Au H, Schlee P, Herou S, Neville T, Cullen P L, Kok M D R, Hosseinaei O, Danielsson S, Tomani P, Titirici M M, Brett D J L, Shearing P R, Jervis R and Jorge A B 2020 *Carbon* **157** 847
[112] Bayeh A W, Kabtamu D M, Chang Y-C, Wondimu T H, Huang H-C and Wang C-H 2021 *Sustainable Energy & Fuels* **5** 1668
[113] Lv Y, Han C, Zhu Y, Zhang T, Yao S, He Z, Dai L and Wang L 2021 *Journal of Materials Science & Technology* **75** 96
[114] Xia L, Long T, Li W, Zhong F, Ding M, Long Y, Xu Z, Lei Y, Guan Y, Yuan D, Zhang Y, Jia C, Sun L and Sun Q 2020 *Small* **16** 2003321